Science Advances
AAAS

Supplementary Materials for

Autocrine inhibition by a glutamate-gated chloride channel mediates presynaptic homeostatic depression

Xiling Li, Chun Chien, Yifu Han, Zihan Sun, Xun Chen, Dion Dickman*

*Corresponding author. Email: dickman@usc.edu

Published 1 December 2021, *Sci. Adv.* **7**, eabj1215 (2021)
DOI: 10.1126/sciadv.abj1215

This PDF file includes:

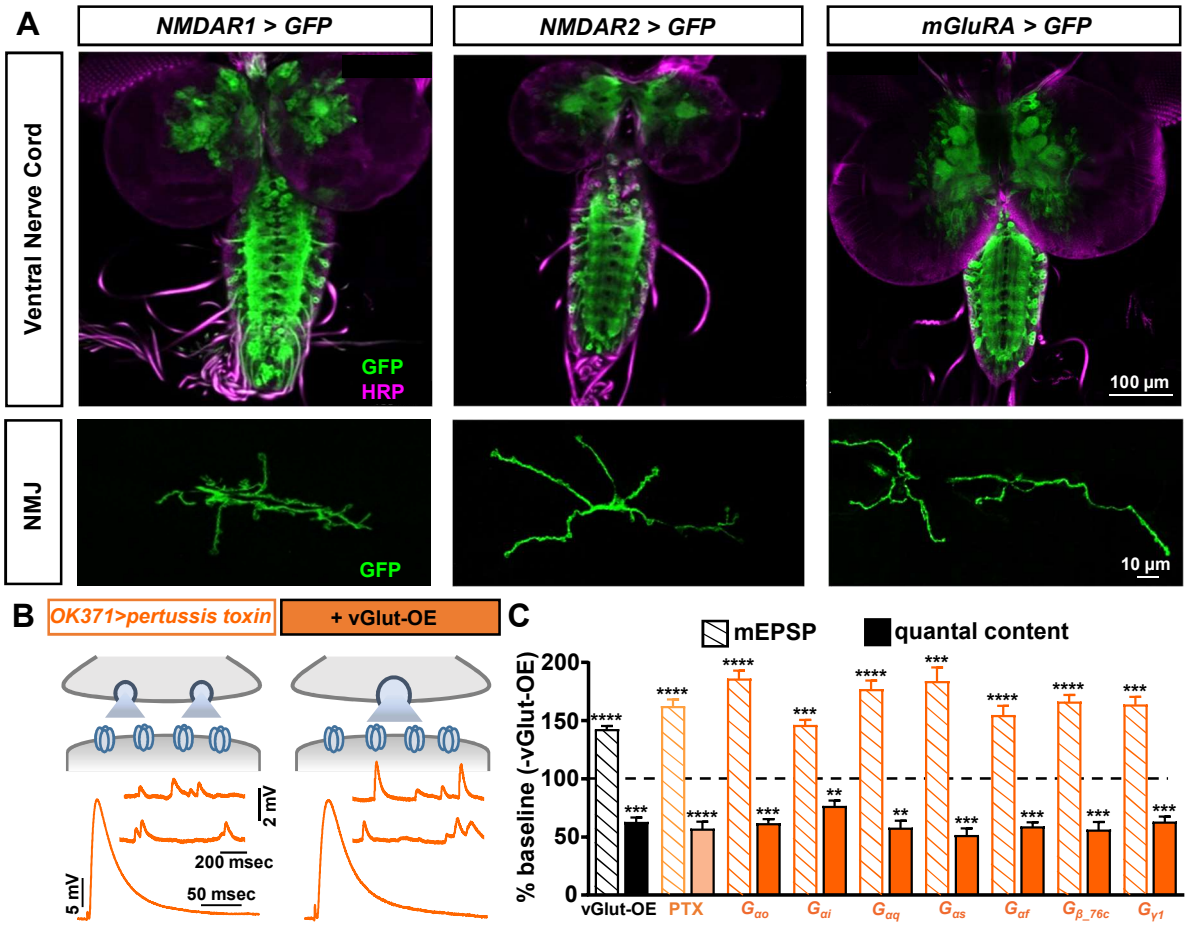

Supplemental Figure 1: Additional screening of metabotropic signaling finds no evidence for roles in PHD. (A) CNS and NMJ single plane confocal images of membrane anchored GFP (CD4::tdGFP; green) and the neuronal membrane marker HRP (magenta) in *NMDAR1>GFP* (*w;NMDAR1-T2A-Gal4/UAS-CD4-td-GFP*), *NMDAR2>GFP* (*NMDAR2-T2A-Gal4;UAS-CD4-td-GFP/+*), and *mGluRA>GFP* (*w; UAS-CD4-td-GFP/+; mGluRA-T2A-Gal4/+*). **(B)** Schematics and representative traces of electrophysiological recordings of pertussis toxin driven in motor neurons (*OK371>pertussis toxin*; *w;OK371-Gal4/+;UAS-pertussis toxin/+*) at baseline and following *vGlut* overexpression (+vGlut-OE: *w;OK371-Gal4/UAS-vGlut;UAS-pertussis toxin/+*). Pertussis toxin disrupts $G_{\alpha i}$ and $G_{\alpha o}$ signaling. **(C)** Quantification of mEPSP and quantal content values normalized to baseline values (-vGlut-OE; n≥8 for all genotypes in this analysis) of all RNAi lines screened targeting G protein signaling. Increased mEPSP amplitudes are observed at all NMJs following *vGlut* overexpression, while a reduction in presynaptic release maintains EPSP amplitude at baseline levels due to PHD expression. Asterisks indicate statistical significance using a Student's t-test: (**) $p<0.01$; (***) $p<0.001$; (****) $p<0.0001$. Error bars indicate ±SEM. n values indicate biologically independent cells. Additional information and absolute values for normalized data can be found in Table S1.

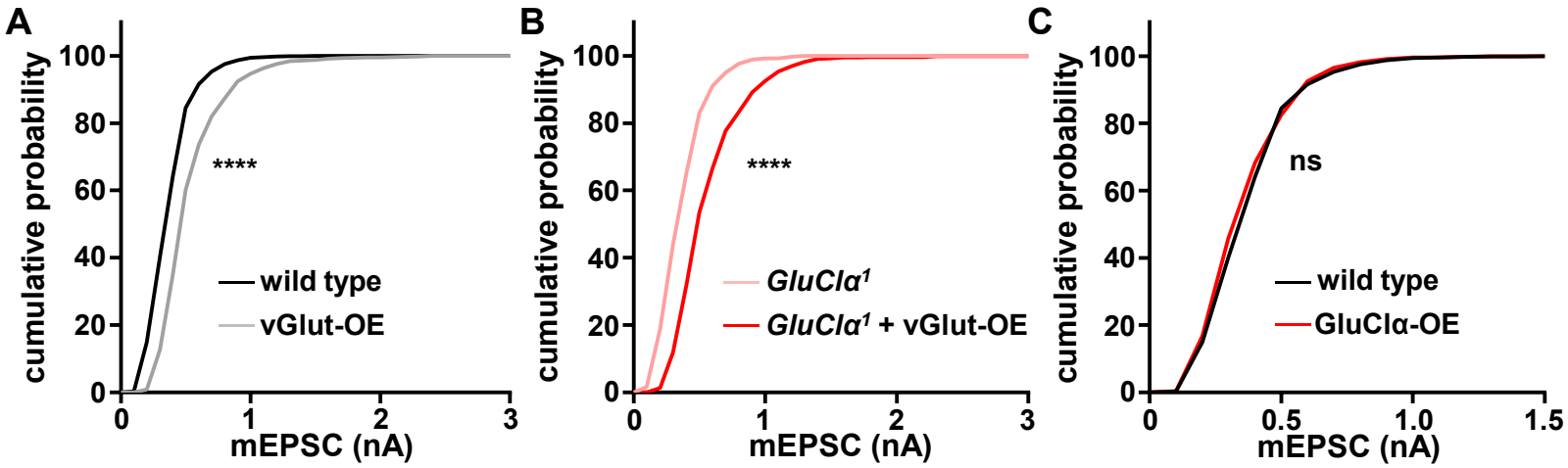

Supplemental Figure 2: vGlut-OE increases miniature amplitude in wild type and *GluClα* mutants. (A) Cumulative probability histogram of mEPSC amplitudes from wild type (w^{1118}, n=908) and vGlut-OE (*w*;*OK371-Gal4/UAS-vGlut,* n=1317) larvae. **(B)** Cumulative probability histogram of mEPSC amplitudes from *GluClα*^{1} (*GluClα*^{1}, n=867) and *GluClα*^{1}+vGlut-OE (*w*;*OK371-Gal4/UAS-vGlut;GluClα*^{1}, n=961) larvae. In both A and B, vGlut-OE significantly enhances the distribution of mEPSC amplitude, as expected. **(C)** Cumulative probability histogram of mEPSC amplitudes from wild type (w^{1118}, n=894) and GluClα^{1}-OE (*w*;*OK371-Gal4/UAS-GluClα,* n=488) larvae. *GluClα* overexpression has no impact on miniature amplitude. Asterisks indicate statistical significance using a Kolmogorov–Smirnov test: (****) $p<0.0001$, (ns) $p>0.05$. n values indicate independent miniature events.

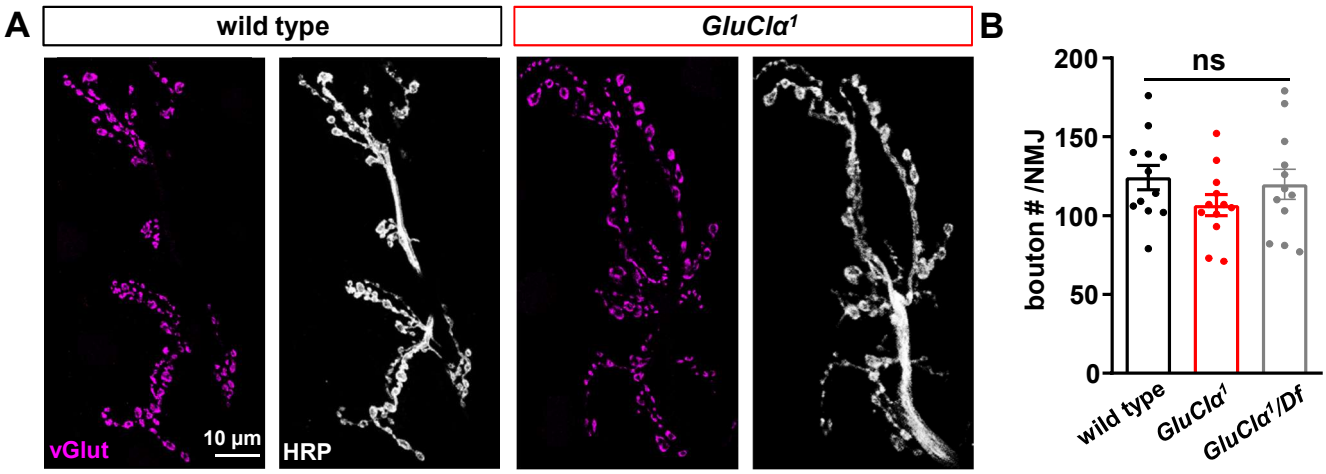

Supplemental Figure 3: *GluClα* mutants exhibit normal synaptic growth. (A) Representative images of muscle 6 and 7 NMJs immunostained with antibodies against the neuronal membrane marker HRP (white) and the glutamate transporter vGlut (magenta) for wild type and *GluClα*^{1}. **(B)** Quantification of bouton number per NMJ in the indicated genotypes. No significant difference in the bouton numbers/NMJ were observed between wild type and *GluClα* mutants. Asterisks indicate statistical significance using a one-way ANOVA followed by multiple comparison: (ns) $p>0.05$. Error bars indicate ±SEM. n values indicate biologically independent cells. Additional information can be found in Table S2.

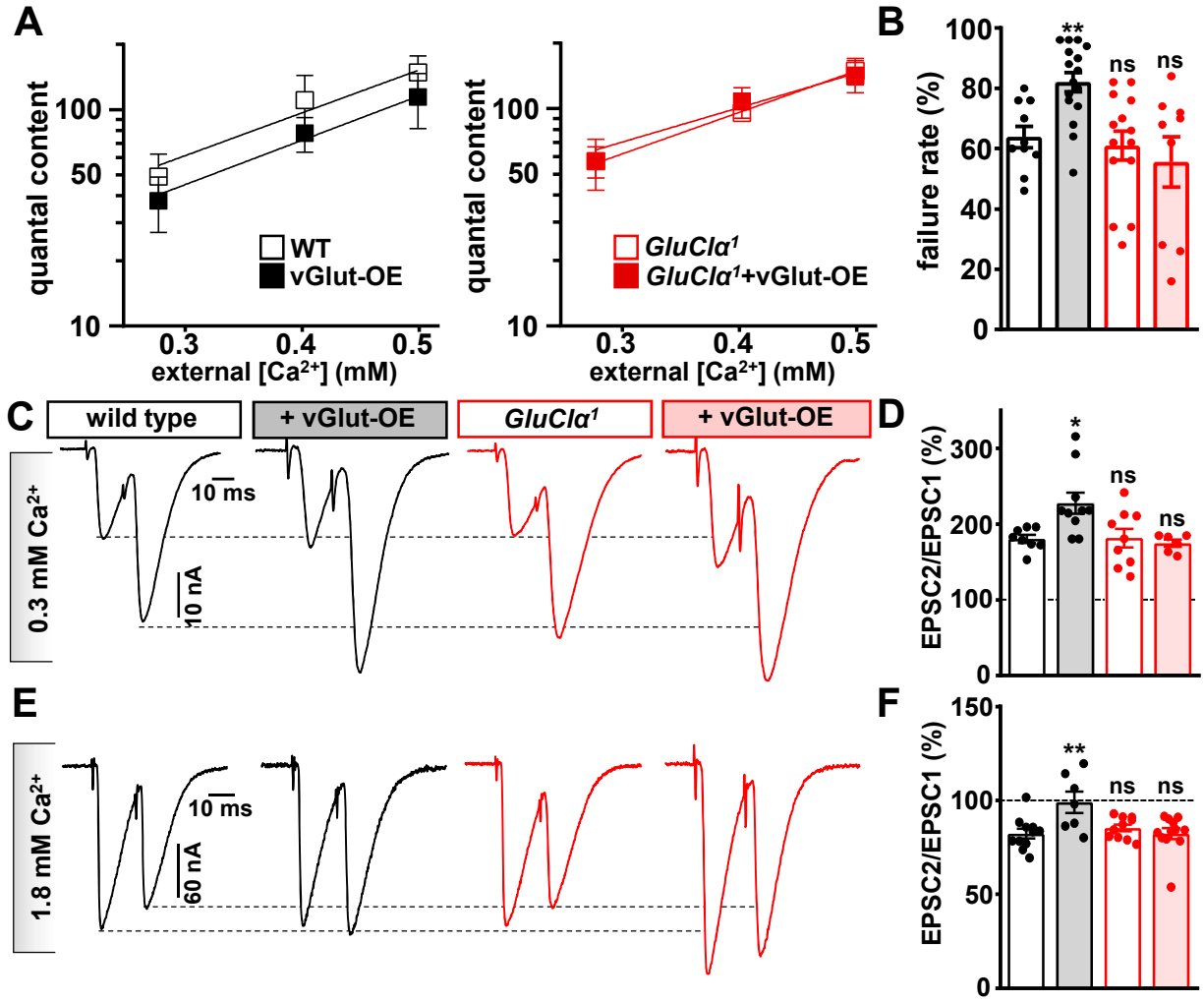

Supplemental Figure 4: Characterization of Ca^{2+} cooperativity, failure analysis and short-term plasticity in *GluClα* mutants. (A) Quantal content plotted as a function of extracellular Ca^{2+} concentration on a log/log scale, with best fit lines shown, for wild type and vGlut-OE and also for *GluClα*^{1} and *GluClα*^{1}+vGlut-OE. No significant difference in the slopes were observed in either graph (Table S2). **(B)** Failure analysis reveals a significant increase in failure rate in vGlut-OE, as expected, due to PHD expression. This increase in failure rate fails to be observed in *GluClα* mutants following *vGlut* overexpression, consistent with a failure to express PHD. **(C)** Representative EPSC traces at 0.3 mM extracellular Ca^{2+} at NMJs of the indicated genotypes stimulated with an interstimulus interval of 16.7 msec. Enhanced paired-pulse facilitation (PPF) was observed at vGlut-OE NMJs, consistent with a decrease in release probability, while this enhancement was not observed in *GluClα*^{1}+vGlut-OE. **(D)** Quantification of the paired-pulse ratio (EPSC2/EPSC1) in the indicated genotypes (wild type n=8, +vGlut-OE n=10; *GluClα*^{1} n=9, +vGlut n=6). **(E)** Representative EPSC traces at 1.8 mM extracellular Ca^{2+} at NMJs of the indicated genotypes stimulated as in (C). No paired-pulse depression (PPD) was observed in vGlut-OE, as expected due to reduced release probability. However, reduced PPD was observed *GluClα*^{1}+vGlut-OE, consistent with a failure to express PHD. **(F)** Quantification of the paired-pulse ratio (EPSC2/EPSC1) in the indicated genotypes (wild type n=11, +vGlut-OE n=7; *GluClα*^{1} n=10, +vGlut-OE n=12). Asterisks indicate statistical significance using a one-way ANOVA followed by multiple comparison: (*) $p<0.05$; (**) $p<0.01$; (ns) $p>0.05$. Error bars indicate ±SEM. n values indicate biologically independent cells. Additional statistical information and absolute values for normalized data can be found in Table S2.

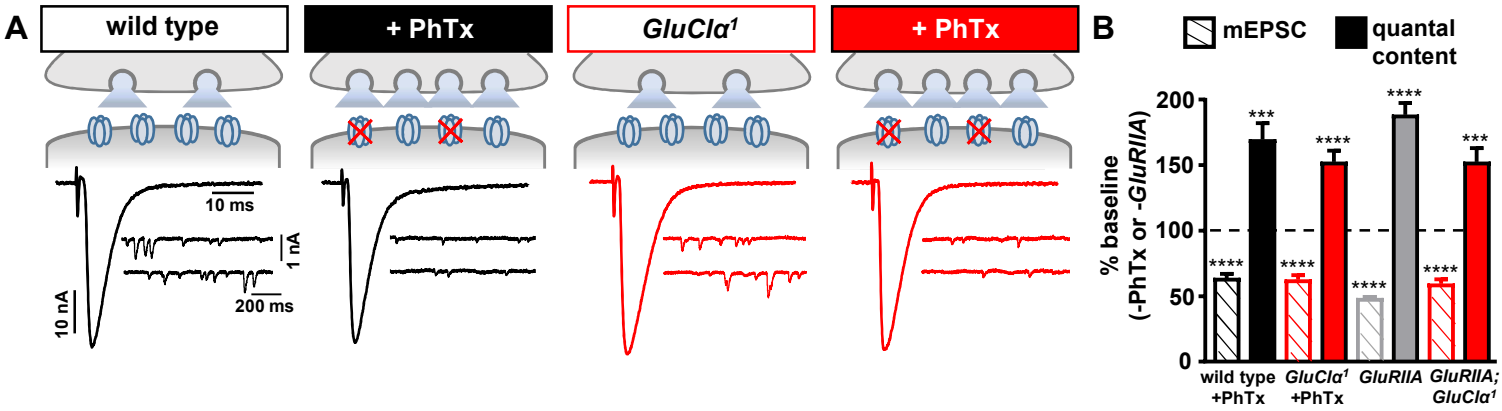

Supplemental Figure 5: *GluClα* is dispensable for PHP expression. (A) Schematics and representative traces of recordings from wild type and *GluClα*^{1} mutant NMJs at baseline and after incubation with the postsynaptic GluR antagonist philanthotoxin-433 (PhTx). mEPSC amplitudes are diminished following PhTx application in both wild-type and *GluClα*^{1} NMJs, as expected, while EPSC amplitudes remain similar to baseline values due to a retrograde enhancement of presynaptic release. Robust PHP expression is observed in both wild type and *GluClα*^{1} mutants. **(B)** Quantification of mEPSC and quantal content values normalized to baseline values in the indicated genotypes (wild type n=11, +PhTx n=9; *GluClα*^{1} n=12, *GluClα*^{1}+PhTx n=8; *GluRIIA*^{sp16} n=6; *GluClα*^{1}+*GluRIIA*^{sp16} n=13). Asterisks indicate statistical significance using a Student's t-test: (***) $p<0.001$; (****) $p<0.0001$. Error bars indicate ±SEM. n values indicate biologically independent cells. Additional statistical information and absolute values for normalized data can be found in Table S2.

Supplementary Table 1: Genes screened for defects in PHD expression and summarized results. The gene information, source, perturbation, electrophysiological values, and number of recordings (n) are shown for each gene screened.

GluR mutations										
CG #	**GluR Gene**	**Abbrev.**	**Allele (s)**	**Source**	**Disruption Type**	**vGlut-OE**	**mEPSP**	**EPSP**	**QC**	**n**
Control			w^{1118}	**wild type**		–	**0.974**	**26.176**	**27.689**	**14**
Control			w^{1118}	**wild type**		+	**1.386**	**23.724**	**17.288**	**15**
3822	Kainate-type ionotropic glutamate receptor subunit 1D	KaiR1D	$DKaiR1D^{1}$	BL18663	tranposon insertion in exonic region	–	1.001	17.026	17.005	9
						+	1.528	16.622	10.882	10
5621	Kainate-type ionotropic glutamate receptor subunit 1C	KaiR1C	$KaiR1C^{MB05324}$	BL24332	tranposon insertion in exonic region	–	0.998	21.709	21.753	9
						+	1.537	23.924	15.792	12
2902	NMDA receptor 1	NMDAR1	$NMDAR1^{XC1}/NMDAR1^{XC3}$	this study	CRISPR/Cas-9 mutagenesis	–	0.912	22.344	26.329	9
						+	1.389	22.659	17.031	10
33513	NMDA receptor 2	NMDAR2	$NMDAR2^{YH7}/Y$	this study	CRISPR/Cas-9 mutagenesis	–	1.115	27.713	24.855	7
						+	1.566	26.184	16.938	8
		NMDAR2	$NMDAR2^{YH7}/NMDAR2^{YH9}$	this study	CRISPR/Cas-9 mutagenesis	–	1.002	28.941	28.939	8
						+	1.31	27.472	21.213	8
11144	metabotropic Glutamate Receptor	mGluRA	$mGluRA^{112b}$	(23)	imprecise P element excision of 5' UTR and coding region	–	0.944	23.542	25.292	9
						+	1.348	24.187	17.819	10
			$mGluRA^{NP6701}$	DGRC105323	tranposon insertion in exonic region	–	0.878	29.736	33.848	8
						+	1.498	28.46	18.997	8
7535	GluClα	GluClα	$GluCl\alpha^{M002890\ (1)}$	BL38025	tranposon insertion in intronic region	–	0.947	27.119	28.642	8
						+	1.42	41.117	29.781	15

GluR RNAi lines										
CG #	**GluR Gene**	**Abb.**	**RNAi**	**Source**	**Genotype**	**vGlut-OE**	**mEPSP**	**EPSP**	**QC**	**n**
11155	CG11155	CG11155	VDRC	VDRC:v11963	$OK371\text{-}Gal4/+;UAS\text{-}RNAi^{GD4652}/+$	–	0.886	26.588	29.993	10
					$OK371\text{-}Gal4/UAS\text{-}vGlut;UAS\text{-}RNAi^{GD4652}/+$	+	1.362	18.921	13.896	8
8681	clumsy	clumsy	VALIUM10	BL28351	$OK371\text{-}Gal4/+;UAS\text{-}TRiP^{JF02987}/+$	–	0.915	24.567	26.849	7
					$OK371\text{-}Gal4/UAS\text{-}vGlut;UAS\text{-}TRiP^{JF02987}/+$	+	1.4363	22.679	15.791	6
5621	Kainate-type ionotropic glutamate receptor subunit 1C	KaiR1C	VALIUM10	BL25822	$OK371\text{-}Gal4/+;UAS\text{-}TRiP^{JF01840}/+$	–	1.027	22.155	21.582	6
					$OK371\text{-}Gal4/UAS\text{-}vGlut;UAS\text{-}TRiP^{JF01840}/+$	+	1.658	16.831	10.391	6
9935	Eye-enriched kainate receptor	Ekar	VALIUM10	BL28506	$OK371\text{-}Gal4/+;UAS\text{-}TRiP^{JF03126}/+$	–	1.078	24.51	23.967	7
					$OK371\text{-}Gal4/UAS\text{-}vGlut;UAS\text{-}TRiP^{JF03126}/+$	+	1.452	14.681	10.394	9
8442	Glutamate receptor IA	GluRIA	VALIUM10	BL27521	$OK371\text{-}Gal4/+;UAS\text{-}TRiP^{JF02671}/+$	–	0.927	26.847	29.489	7
					$OK371\text{-}Gal4/UAS\text{-}vGlut;UAS\text{-}TRiP^{JF02671}/+$	+	1.301	25.439	19.985	7
43743	Glutamate receptor IB	GluRIB	VALIUM10	BL27673	$OK371\text{-}Gal4/+;UAS\text{-}TRiP^{JF02752}/+$	–	1.049	24.278	23.284	6
					$OK371\text{-}Gal4/UAS\text{-}vGlut;UAS\text{-}TRiP^{JF02752}/+$	+	1.564	19.649	12.811	11
2902	NMDA receptor 1	NMDAR1	VALIUM10	BL25941	$OK371\text{-}Gal4/+;UAS\text{-}TRiP^{JF01961}/+$	–	0.853	26.629	31.497	8
					$OK371\text{-}Gal4/UAS\text{-}vGlut;UAS\text{-}TRiP^{JF01961}/+$	+	1.218	18.11	14.867	11
33513	NMDA receptor 2	NMDAR2	VALIUM10	BL26019	$OK371\text{-}Gal4/+;UAS\text{-}TRiP^{JF02044}/+$	–	1.021	31.386	31.573	18
					$OK371\text{-}Gal4/UAS\text{-}vGlut;UAS\text{-}TRiP^{JF02044}/+$	+	1.273	29.767	23.921	16
		NMDAR2	VALIUM20	BL40846	$OK371\text{-}Gal4/+;UAS\text{-}TRiP^{HMS02012}/+$	–	1.017	25.099	24.688	7
					$OK371\text{-}Gal4/UAS\text{-}vGlut;UAS\text{-}TRiP^{HMS02012}/+$	+	1.291	20.798	16.411	8

RNAi lines targeting metabotropic signaling										
CG #	**Gene**	**Abb.**	**disruption type**	**Source**	**Genotype**	**vGlut-OE**	**mEPSP**	**EPSP**	**QC**	**n**
Control			w^{1118}	**wild type**		–	**0.896**	**26.553**	**30.023**	**11**
10060	G protein α i subunit	Gαi	VALIUM1	BL31133	$OK371\text{-}Gal4/UAS\text{-}vGlut;UAS\text{-}RNAi^{JF01608}/+$	+	1.281	28.558	22.311	8
		Gαi	VALIUM20	BL34924	$OK371\text{-}Gal4/UAS\text{-}vGlut;UAS\text{-}RNAi^{HMS01273}/+$	+	1.267	26.298	20.88	6
2204	G protein α o subunit	Gαo	VALIUM10	BL28010	$OK371\text{-}Gal4/UAS\text{-}vGlut;UAS\text{-}RNAi^{JF02844}/+$	+	1.836	28.771	15.706	6
17759	G protein α q subunit	Gαq	VALIUM20	BL36775	$OK371\text{-}Gal4/UAS\text{-}vGlut;UAS\text{-}RNAi^{JF02390}/+$	+	1.451	25.427	18.046	8
2835	G protein α s subunit	Gαs	VALIUM20	BL50704	$OK371\text{-}Gal4/UAS\text{-}vGlut;UAS\text{-}RNAi^{HMC03106}/+$	+	1.507	23.155	16.079	8
12232	G protein α f subunit	Gαf	VALIUM10	BL25930	$OK371\text{-}Gal4/UAS\text{-}vGlut;UAS\text{-}RNAi^{JF01950}/+$	+	1.449	24.264	17.106	8
8770	G protein β-subunit 76C	Gβ 76C	VALIUM10	BL28507	$OK371\text{-}Gal4/UAS\text{-}vGlut;UAS\text{-}RNAi^{JF03127}/+$	+	1.074	23.588	22.979	8
8261	G protein γ 1	Gγ1	VALIUM10	BL25934	$OK371\text{-}Gal4/UAS\text{-}vGlut;UAS\text{-}RNAi^{JF01954}/+$	+	1.342	26.501	19.724	7

Supplementary Table 2: Absolute values for normalized data and additional statistical details. The figure and panel, genotype, and conditions are noted. Average values (with standard error values noted in parentheses) are shown for all data. For electrophysiological experiments, passive membrane properties (input resistance, leak current), mEPSC, EPSC, quantal content (QC), data samples (n), and statistical significance tests and values are shown.

Figure	Label	Genotype	$[Ca^{2+}]$ mM	vGlut-OE	mEPSC amplitude (nA)	EPSC amplitude (nA)	QC	mEPSC frequency (Hz)	R_{input} (MΩ)	leak current (nA)	n	P Value (significance: mEPSC amp, EPSC, QC)
Figure 2D-G	wild type	*w^{1118}*	0.4	-	0.438 (±0.012)	41.285 (±3.239)	105.890 (±8.018)	2.360 (±0.464)	6.000 (±0.588)	–1.693 (±0.275)	18	-
Figure 2D-G	vGlut-OE	*w;OK371-Gal4/UAS-vGlut*	0.4	+	0.597 (±0.022)	44.085 (±2.523)	71.950 (±4.248)	1.886 (±0.272)	7.333 (±0.267)	–2.695 (±0.230)	19	<0.0001 (****), 0.4971 (ns), 0.0006 (***)
Figure 2D-G	*GluClα^{1}*	*w;GluClα^{1}*	0.4	-	0.487 (±0.022)	40.724 (±3.653)	86.422 (±9.351)	2.283 (±0.187)	6.800 (±0.693)	–1.718 (±0.301)	13	-
Figure 2D-G	*GluClα^{1}* + vGlut-OE	*w;OK371-Gal4/UAS-vGlut;GluClα^{1}*	0.4	+	0.655 (±0.019)	66.203 (±4.759)	101.606 (±7.492)	2.542 (±0.201)	8.000 (±0.803)	–2.481 (±0.264)	10	<0.0001 (****), 0.0002 (***), 0.3832 (ns)
Figure 2G	*GluClα^{1}/Df*	*w;GluClα^{1}/Df(BSC809)*	0.4	-	0.442 (±0.011)	39.178 (±3.667)	90.339 (±9.912)	2.252 (±0.144)	8.545 (±0.731)	–-2.848 (±0.424)	11	-
Figure 2G	*GluClα^{1}/Df* + vGlut-OE	*w;OK371-Gal4/UAS-vGlut;GluClα^{1}/Df^{BSC809}*	0.4	+	0.572 (±0.015)	53.939 (±2.349)	94.876 (±4.848)	3.003 (±0.722)	7.900 (±0.314)	–2.175 (±0.389)	10	<0.0001 (****), 0.0037 (**), 0.6949 (ns)
Figure 2G	*GluClα^{glc}/Df*	*w;GluClα^{glc}/Df^{BSC809}*	0.4	-	0.435 (±0.022)	42.784 (±3.918)	101.577 (±10.776)	2.252 (±0.144)	8.235 (±0.683)	–-2.133 (±0.316)	13	-
Figure 2G	*GluClα^{glc}/Df* + vGlut-OE	*w;OK371-Gal4/UAS-vGlut;GluClα^{glc}/Df^{BSC809}*	0.4	+	0.562 (±0.013)	61.426 (±3.609)	108.893 (±4.497)	3.276 (±0.445)	10.429 (±0.922)	–2.089 (±0.281)	7	0.0007 (***), 0.0060 (**), 0.6364 (ns)
Figure 2G	*GluClα$^{FlpStop.D}$*	*w;GluClα$^{FlpStop.D}$*	0.4	-	0.443 (±0.023)	43.473 (±0.821)	99.736 (±3.821)	3.473 (±0.443)	10.000 (±0.724)	–2.427 (±0.453)	10	-
Figure 2G	*GluClα$^{FlpStop.D}$* + vGlut-OE	*w;OK371-Gal4/UAS-vGlut;GluClα$^{FlpStop.D}$*	0.4	+	0.628 (±0.026)	56.778 (±1.840)	91.297 (±3.074)	3.441 (±0.424)	10.024 (±0.759)	–2.057 (±0.244)	11	<0.0001 (****), <0.0001 (****), 0.0989 (ns)
Figure 2	wild type	*w^{1118}*	0.4	-	0.442 (±0.015)	42.938 (±3.354)	98.336 (±9.300)	3.315 (±0.386)	8.500 (±0.627)	-2.642 (±0.477)	8	
Figure 2	*Df*/+	*w;Df(BSC809)/+*	0.4	-	0.438 (±0.028)	43.012 (±4.406)	100.790 (±13.215)	2.142 (±0.415)	7.167 (±0.601)	-1.097 (±)	6	0.9306 (ns), 0.9893 (ns), 0.8913 (ns)
Figure 2	*GluClα^{1}/+*	*w;GluClα^{1}/+*	0.4	-	0.437 (±0.013)	39.002 (±2.721)	89.218 (±6.010)	3.145 (±0.217)	7.000 (±0.535)	-1.591 (±0.329)	7	0.7993 (ns), 0.3877 (ns), 0.4401 (ns)
Figure 2	*GluClα^{glc}/+*	*w;GluClα^{glc}/+*	0.4	-	0.482 (±0.017)	40.665 (±3.665)	84.513 (±7.166)	4.000 (±0.574)	7.667 (±0.760)	-3.168 (±0.185)	6	0.0980 (ns), 0.6582 (ns), 0.2889 (ns)
Figure 2	*GluClα$^{FlpStop.D}$/+*	*w;GluClα$^{FlpStop.D}$/+*	0.4	-	0.474 (±0.016)	42.062 (±5.336)	90.468 (±13.621)	3.381 (±0.309)	8.286 (±0.837)	-2.049 (±0.160)	7	0.1624 (ns), 0.8886 (ns), 0.6340 (ns)
Figure 3B,C	wild type	*w^{1118}*	0.4	-	0.417 (±0.009)	40.901 (±3.381)	98.024 (±7.943)	3.681 (±0.215)	7.667 (±0.607)	–2.205 (±0.181)	12	-
Figure 3B,C	vGlut-OE	*w;OK371-Gal4/UAS-vGlut*	0.4	+	0.605 (±0.023)	36.980 (±1.541)	61.801 (±3.001)	2.892 (±0.278)	7.923 (±0.665)	–1.875 (±0.214)	13	<0.0001 (****), 0.2897 (ns), 0.0002 (***)
Figure 3B,C	pre > GluClα RNAi	*w;OK371-Gal4/UAS-GluClα RNAi;UAS-Dcr2/+*	0.4	-	0.404 (±0.008)	43.862 (±1.712)	109.718 (±5.309)	1.705 (±0.183)	8.813 (±0.736)	–2.743 (±0.326)	16	-
Figure 3B,C	pre > GluClα RNAi + vGlut-OE	*w;OK371-Gal4/UAS-vGlut,UAS-GluClα RNAi;UAS-Dcr2/+*	0.4	+	0.567 (±0.011)	69.073 (±1.756)	122.648 (±3.669)	2.262 (±0.223)	8.250 (±0.491)	–1.687 (±0.219)	20	<0.0001 (****), <0.0001 (****), 0.0544 (ns)

Figure	Label	Genotype	$[Ca^{2+}]$ mM	extracellular Cl^-	mEPSC amplitude (nA)	EPSC amplitude (nA)	QC	mEPSC frequency (Hz)	input resistance (MΩ)	leak current (nA)	n	P Value (significance: mEPSC amp, EPSC, QC)
Figure 4A-E	wild type	*w^{1118}*	0.4	+	0.448 (±0.010)	45.194 (±3.169)	101.676 (±7.407)	3.199 (±0.277)	8.200 (±0.460)	–2.063 (±0.344)	15	-
Figure 4A-E	vGlut-OE	*w;OK371-Gal4/UAS-vGlut*	0.4	+	0.572 (±0.026)	40.122 (±1.442)	72.018 (±3.927)	2.516 (±0.350)	6.941 (±0.433)	–2.386 (±0.205)	17	0.0002 (***), 0.140 (ns), 0.0009 (***)
Figure 4A-E	wild type (Cl^- free)	*w^{1118}*	0.4	-	0.409 (±0.009)	40.744 (±4.275)	101.324 (±12.022)	3.587 (±0.285)	8.250 (±0.708)	–4.518 (±0.406)	12	-
Figure 4A-E	vGlut-OE (Cl^- free)	*w;OK371-Gal4/UAS-vGlut*	0.4	-	0.493 (±0.015)	57.275 (±3.984)	117.675 (±8.737)	2.207 (±0.381)	6.071 (±0.425)	–3.601 (±0.295)	13	0.0001 (***), 0.0094 (**), 0.2773 (ns)

Figure	Label	Genotype	$[Ca^{2+}]$ mM	mEPSC amplitude (nA)	EPSC amplitude (nA)	QC	mEPSC frequency (Hz)	input resistance (MΩ)	leak current (nA)	n	P Value (significance: mEPSC amp, EPSC, QC)
Figure 5B-D	wild type	*w^{1118}*	0.4	0.475 (±0.014)	42.845 (±1.785)	91.322 (±4.619)	3.571 (±0.403)	7.000 (±0.516)	–2.107 (±0.320)	13	-
Figure 5B-D	pre > GluClα	*w;OK371-Gal4/UAS-GluClα*	0.4	0.468 (±0.015)	29.983 (±1.783)	66.873 (±4.994)	2.527 (±0.183)	7.833 (±0.442)	–1.853 (±0.245)	26	0.7632 (ns), <0.0001 (****), 0.0017 (**)
Figure 5	wild type	*w^{1118}*	0.4	0.474 (±0.017)	48.819 (±2.332)	103.590 (±4.764)	3.041 (±0.306)	8.333 (±0.699)	–2.381 (±0.369)	13	
Figure 5	pre > GluClα::smFP	*w;OK371-Gal4/UAS-GluClα::smFP*	0.4	0.437 (±0.021)	30.803 (±3.245)	75.740 (±9.234)	3.346 (±0.182)	10.391 (±1.494)	–2.366 (±0.223)	21	0.2190 (ns), 0.0004 (***), 0.0314 (*)

Figure	Label	Genotype	$[Ca^{2+}]$ mM	τ_{rise} (% baseline - ivermectin)	τ_{decay} (% baseline -ivermectin)	mEPSC area (% baseline -ivermectin)	QC (% baseline -ivermectin)	leak current (nA)	n	P value (τ_{rise}, τ_{decay}, mEPSC area, QC comapre to baseline - ivermectin)
Figure 6B-E	wild type	*w^{1118}*	0.4	101.725 (±2.939)	72.724 (±3.855)	95.952 (±6.256)	75.591 (±3.413)	–2.782 (±0.699)	5	0.0685 (ns), 0.0002 (***), 0.7956 (ns), 0.0032 (**)
Figure 6B-E	*GluClα^{1}*	*w;GluClα^{1}*	0.4	98.973 (±1.626)	96.017 (±3.417)	96.651 (±7.1679)	97.002 (±5.589)	–2.077 (±0.844)	5	0.4140 (ns), 0.3002 (ns), 0.6466 (ns), 0.6888 (ns)
Figure 6B-E	*vGlut-OE*	*w;OK371-Gal4/UAS-vGlut*	0.4	97.867 (±1.671)	84.090 (±2.445)	97.832 (±8.820)	63.068 (±5.987)	–1.738 (±0.965)	7	0.2109 (ns), 0.0011 (**), 0.8846 (ns), 0.0003 (***)

Figure	Label	Genotype	Triton	mean intensity (AU, Arbitrary Unit)			n	P Value (significance: mean intensity)
				vGlut	GluClα	Syt		
Figure 7B	GluClα-OE	*w;OK371-Gal4/ UAS-GluClα::smFP*	+	713.187 (±26.36)	509.365 (±28.903)	1114.043 (±48.263)	24	-
Figure 7B	GluClα-OE + vGlut-OE	*w;OK371-Gal4/UAS-vGlut,UAS-GluClα::smFP*	+	1232.932 (±65.171)	651.480 (±37.405)	713.187 (±97.701)	22	<0.0001 (****), 0.0136 (*), 0.1284 (ns)
Figure 7D	GluClα-OE	*w;OK371-Gal4/ UAS-GluClα::smFP*	-	52.057 (±3.575)	97.654 (±6.648)	86.882 (±5.865)	16	<0.0001 (****), <0.0001 (****), <0.0001 (****) Compare to - Triton
Figure 7D	GluClα-OE + vGlut-OE	*w;OK371-Gal4/UAS-vGlut,UAS-GluClα::smFP*	-	84.760 (±8.399)	98.098 (±6.504)	77.703 (±5.584)	16	<0.0001 (****), <0.0001 (****), <0.0001 (****) Compare to - Triton

Figure	Label	Genotype	Triton	high K+	temp	mean intensity (AU, Arbitrary Unit)			n	P Value (significance: mean intensity)
						vGlut	GluClα	Syt		
Figure 7F	*shi*:GluClα-OE	*shi^{ts1}/y; OK371-Gal4/ UAS-GluClα::smFP*	-	-	RT	98.267 (±13.221)	190.432 (±28.278)	144.144 (±29.954)	11	-
Figure 7F	*shi*:GluClα-OE	*shi^{ts1}/y; OK371-Gal4/ UAS-GluClα::smFP*	-	+	34℃	86.303 (±9.942)	348.23 (±31.109)	136.37 (±17.850)	13	0.1071 (ns), 0.0018 (**), 0. 8272 (ns)

Figure	Label	Genotype	$[Ca^{2+}]$ mM	extracellular Cl^-	ΔR/ R	τ_{decay} (s)	rise time (ms)	n	P value (ΔR/ R, τ_{decay} (s), and rise time comapre to wild type control)
Figure 8C-D	wild type	*w^{1118}*	1.0	+	0.617 (±0.043)	0.206 (±0.011)	13.202 (±0.954)	12	-
Figure 8C-D	vGlut-OE	*w;OK371-Gal4/UAS-vGlut*	1.0	+	0.298 (±0.019)	0.214 (±0.009)	12.752 (±0.485)	12	<0.0001 (****), 0.6224 (ns), 0.6783 (ns)
Figure 8E-F	wild type (Cl^- free)	*w^{1118}*	1.0	-	0.592 (±0.022)	0.215 (±0.008)	12.739 (±0.571)	12	-
Figure 8E-F	vGlut-OE (Cl^- free)	*w;OK371-Gal4/UAS-vGlut*	1.0	-	0.615 (±0.040)	0.206 (±0.009)	13.422 (±0.669)	12	0.6192 (ns), 0.4422 (ns), 0.4456 (ns)

Figure	Label	Genotype	$[Ca^{2+}]$ mM	vGlut-OE	mEPSP amplitude (mV)	EPSP amplitude (mV)	QC	mEPSP frequency (Hz)	input resistance (MΩ)	resting potential (mV)	n	P Value (significance: mEPSC amp, EPSC, QC)
Supplemental Figure 1B,C	pertussis toxin	*w;OK371-Gal4/+;UAS-PTX/+*	0.3	-	0.872 (±0.088)	17.883 (±2.105)	19.505 (±1.305)	0.872 (±0.088)	8.000 (±0.405)	–64.069 (±2.449)	11	-
Supplemental Figure 1B,C	pertussis toxin	*w;OK371-Gal4/UAS-vGlut;UAS-PTX/+*	0.3	+	1.415 (±0.051)	15.636 (±1.827)	11.046 (±1.262)	2.563 (±0.264)	7.889 (±0.716)	–63.614 (±0.836)	9	<0.0001 (****), 0.4420 (ns), 0.0002 (***)

Figure	Label	Genotype	bouton #/NMJ	n	P Value (significance: mEPSC amp, EPSC, QC)
Supplemental Figure 3B	wild type	*w^{1118}*	124.167 (±7.813)	12	-
Supplemental Figure 3B	*GluClα^{1}*	*w;GluClα^{1}*	106.750 (±6.609)	12	0.2958 (ns)
Supplemental Figure 3B	*GluClα^{1}/Df*	*w;GluClα^{1}/DF^{BSC809}*	119.833 (±9.634)	12	0.9246 (ns)

Figure	Label	Genotype	$[Ca^{2+}]$ mM	QC	Ca^{2+} coop slope	input resistance (MΩ)	leak current (nA)	n	P Value (significance: slope)
Supplemental Figure 4A	wild type	*w^{1118}*	0.3	49.185 (±3.624)	1.980 (R^2: 0.745)	8.000 (±0.577)	–3.411 (±0.652)	13	-
Supplemental Figure 4A	vGlut-OE	*w;OK371-Gal4/UAS-vGlut*	0.3	37.929 (±3.625)	2.051 (R^2: 0.692)	11.333 (±1.054)	–2.997 (±0.353)	9	0.8704 (ns)
Supplemental Figure 4A	*GluClα^{1}*	*w;GluClα^{1}*	0.3	57.262 (±5.735)	1.910 (R^2: 0.868)	5.571 (±0.481)	–2.205 (±0.224)	7	-
Supplemental Figure 4A	*GluClα^{1}* + vGlut-OE	*w;OK371-Gal4/UAS-vGlut;GluClα^{1}*	0.3	57.337 (±3.847)	1.585 (R^2: 0.744)	6.500 (±0.671)	–1.517 (±0.409)	6	0.2755 (ns)

Supplemental Figure 4A	wild type	w^{1118}	0.4	108.049 (±11.798)	–	6.500 (±0.535)	–3.266 (±0.296)	8	-
Supplemental Figure 4A	vGlut-OE	*w;OK371-Gal4/UAS-vGlut*	0.4	77.826 (±5.821)	–	7.333 (±0.422)	–3.691 (±0.433)	6	-
Supplemental Figure 4A	$GluCl\alpha^{1}$	*w;GluClα*^{1}	0.4	95.295 (±3.25)	–	5.167 (±0.307)	–2.149 (±0.189)	6	-
Supplemental Figure 4A	$GluCl\alpha^{1}$ + vGlut-OE	*w;OK371-Gal4/UAS-vGlut;GluClα*^{1}	0.4	107.684 (±5.161)	–	7.182 (±0.724)	–1.327 (±0.264)	11	-
Supplemental Figure 4A	wild type	w^{1118}	0.5	148.632 (±8.679)	–	7.364 (±0.704)	–2.033 (±0.265)	11	-
Supplemental Figure 4A	vGlut-OE	*w;OK371-Gal4/UAS-vGlut*	0.5	114.442 (±9.851)	–	10.636 (±0.917)	–2.218 (±0.302)	11	-
Supplemental Figure 4A	$GluCl\alpha^{1}$	*w;GluClα*^{1}	0.5	149.193 (±6.942)	–	11.556 (±1.180)	–1.474 (±0.136)	9	-
Supplemental Figure 4A	$GluCl\alpha^{1}$ + vGlut-OE	*w;OK371-Gal4/UAS-vGlut;GluClα*^{1}	0.5	142.385 (±7.990)	–	11.222 (±0.795)	–2.091 (±0.389)	9	-

Figure	Label	Genotype	$[Ca^{2+}]$ mM	failure rate (%)	input resistance (MΩ)	resting potential (mV)	n	P Value (significance: failure rate)
Supplemental Figure 4B	wild type	w^{1118}	0.1	55.556 (±8.352)	10.778 (±0.830)	–66.645 (±0.606)	9	-
Supplemental Figure 4B	vGlut-OE	*w;OK371-Gal4/UAS-vGlut*	0.1	82.000 (±3.220)	14.875 (±0.676)	–67.221 (±1.425)	16	0.0019 (**)
Supplemental Figure 4B	$GluCl\alpha^{1}$	*w;GluClα*^{1}	0.1	61.000 (±4.775)	10.571 (±0.510)	–67.411 (±1.173)	14	0.5486 (ns)
Supplemental Figure 4B	$GluCl\alpha^{1}$ + vGlut-OE	*w;OK371-Gal4/UAS-vGlut;GluClα*^{1}	0.1	63.800 (±3.608)	10.200 (±0.573)	–67.294 (±1.592)	10	0.3604 (ns)

Figure	Label	Genotype	$[Ca^{2+}]$ mM	paired-pulse rate (%)	input resistance (MΩ)	leak current (nA)	n	P Value (significance: paired-pulse rate)
Supplemental Figure 4D	wild type	w^{1118}	0.3	180.462 (±5.188)	7.250 (±0.491)	–4.913 (±0.791)	8	-
Supplemental Figure 4D	vGlut-OE	*w;OK371-Gal4/UAS-vGlut*	0.3	227.726 (±13.939)	11.200 (±0.952)	–3.462 (±0.398)	10	0.0106 (*)
Supplemental Figure 4D	$GluCl\alpha^{1}$	*w;GluClα*^{1}	0.3	181.601 (±12.461)	7.111 (±1.006)	–2.214 (±1.486)	9	0.9427 (ns)
Supplemental Figure 4D	$GluCl\alpha^{1}$ + vGlut-OE	*w;OK371-Gal4/UAS-vGlut;GluClα*^{1}	0.3	174.701 (±4.814)	6.500 (±0.671)	–1.790 (±0.446)	6	0.4463 (ns)
Supplemental Figure 4F	wild type	w^{1118}	1.8	82.348 (±2.590)	9.091 (±0.879)	–0.011 (±0.002)	11	-
Supplemental Figure 4F	vGlut-OE	*w;OK371-Gal4/UAS-vGlut*	1.8	99.042 (±5.676)	10.143 (±1.100)	0.001 (±0.0004)	7	0.0081 (**)
Supplemental Figure 4F	$GluCl\alpha^{1}$	*w;GluClα*^{1}	1.8	85.383 (±1.844)	11.100 (±0.781)	–0.013 (±0.003)	10	0.3601 (ns)
Supplemental Figure 4F	$GluCl\alpha^{1}$ + vGlut-OE	*w;OK371-Gal4/UAS-vGlut;GluClα*^{1}	1.8	82.375 (±2.890)	13.083 (±0.821)	–0.007 (±0.001)	12	0.9947 (ns)

Figure	Label	Genotype	[Ca^{2+}] mM	PhTx	mEPSC amplitude (nA)	EPSC amplitude (nA)	QC	mEPSP frequency (Hz)	input resistance (MΩ)	leak current (nA)	n	P Value (significance: mEPSC amp, EPSC, QC)
Supplemental Figure 5B	wild type	w^{1118}	0.4	-	0.439 (±0.016)	42.514 (±3.658)	96.730 (±7.981)	3.415 (±0.364)	9.909 (±1.187)	–2.346 (±0.419)	11	-
Supplemental Figure 5B	wild type	w^{1118}	0.4	+	0.281 (±0.012)	45.212 (±2.469)	164.033 (±12.230)	2.254 (±0.211)	11.556 (±0.801)	–2.079 (±0.251)	9	<0.0001 (****), 0.5674 (ns), 0.0002 (***)
Supplemental Figure 5B	*GluRIIA*	*w;GluRIIA^{SP16}*	0.4	-	0.213 (±0.005)	38.843 (±2.091)	182.379 (±8.581)	0.787 (±0.096)	7.167 (±0.307)	–1.435 (±0.206)	6	<0.0001 (****), 0.4948 (ns), <0.0001 (****)
Supplemental Figure 5B	*GluClα^{1}*	*w;GluClα^{1}*	0.4	-	0.419 (±0.011)	47.805 (±2.750)	115.077 (±7.238)	3.014 (±0.391)	9.250 (±0.351)	–2.336 (±0.282)	12	-
Supplemental Figure 5B	*GluClα^{1}*	*w;GluClα^{1}*	0.4	+	0.263 (±0.014)	46.114 (±3.462)	175.624 (±9.821)	2.304 (±0.191)	9.500 (±0.945)	–3.156 (±0.771)	8	<0.0001 (****), 0.7049 (ns), <0.0001 (****)
Supplemental Figure 5B	*GluClα^{1} + GluRIIA*	*w;GluRIIA^{SP16}; GluClα^{1}*	0.4	-	0.249 (±0.015)	42.035 (±1.627)	175.492 (±12.152)	2.530 (±0.256)	11.539 (±0.938)	–4.204 (±0.163)	13	<0.0001 (****), 0.0787 (ns), 0.0004 (***)

Supplementary Table 3: Key resources table.

REAGENT or RESOURCE	SOURCE	IDENTIFIER
Chemicals, Peptides, and Recombinant Proteins		
Ivermectin	Sigma-Aldrich	I8898-250MG, CAS: 70288-86-7
Philanthotoxin 433	Sigma-Aldrich	CAS: 276684-27-6
Methyl sulfate sodium salt	Sigma-Aldrich	318183-25G, CAS: 512-42-5
Potassium methaesulfonate	Sigma-Aldrich	83000-5G-F, CAS: 2386-56-3
Magnesium nitrate hexahydrate	Sigma-Aldrich	63084-500G-F, CAS: 13446-18-9
Calcium nitrate tetrahydrate	Sigma-Aldrich	C1396-500G, CAS: 13477-34-4
Antibodies		
Mouse anti-Flag	Sigma-Aldrich	F1804
Phalloidin-Alexa Fluor 647	Thermo Fisher	A22287
Guinea pig anti-vGlut	(66)	
Rabbit anti-Synaptotagmin	(67)	
Alexa Fluor 647 conjugated Goat anti-Horseradish Peroxidase	Jackson ImmunoResearch Labs	123-605-021
Alexa Fluor 488-conjugated secondary antibodies	Jackson ImmunoResearch Labs	706-545-148, 715-545-150, 711-545-152
Cy3-conjugated secondary antibodies	Jackson ImmunoResearch Labs	706-165-148, 715-165-150, 711-165-152
DyLight 405-conjugated secondary antibodies	Jackson ImmunoResearch Labs	715-475-150, 706-475-148, 711-475-152
Experimental Models: *D. melanogaster* Strains		
OK371-Gal4	Mahr et al., 2006	
UAS-vGlut	(11)	
UAS-GluClα-RNAi p{KK109167}VIE-260B	VDRC	v105754
UAS-CD4::tdeGFP	Han et al., 2011	
UAS-Dcr2	BDSC	24651
$GluCl\alpha^{MI02890}$	BDSC	38025
$GluCl\alpha^{glc}$	BDSC	6353
$GluCl\alpha^{FlpStop.D}$	(38)	
GluClα-T2A-Gal4	(40)	
mGluRA-T2A-Gal4	(40)	
NMDAR1-T2A-Gal4	(40)	
NMDAR2-T2A-Gal4	(40)	
Df(3R)BSC809	BDSC	27380
UAS-GluClα	This study	
UAS-GluClα::smFP	This study	
$shibire^{ts1}$	BDSC	7068
UAS-Syt::mScar::GCaMP8f	This study	
Software and Algorithms		
NIS Elements software	Nikon	4.51.01
Axon pCLAMP Clampfit	Molecular Devices	10.7
MiniAnalysis	Synaptosoft	6.0.3
Excel	Microsoft	2016
SigmaPlot	Systat	14
GraphPad Prism	GraphPad	8.0.1